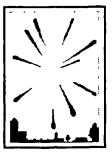

Meteoritics & Planetary Science 37, 1711–1728 (2002)
Available online at http://www.uark.edu/meteor

Cosmogenic nuclides in the Brenham pallasite

M. HONDA[1], M. W. CAFFEE[2†], Y. N. MIURA[3], H. NAGAI[1], K. NAGAO[4‡] AND K. NISHIIZUMI[5*]

[1]Department of Chemistry, Nihon University, Setagaya, Tokyo 156-8550, Japan
[2]Center for Accelerator Mass Spectrometry, Lawrence Livermore National Laboratory, Livermore, California 94550, USA
[3]Earthquake Research Institute, University of Tokyo, Tokyo 113-0032, Japan
[4]Institute for Study of the Earth's Interior, Okayama University, Misasa, Tottori 682-0193, Japan
[5]Space Sciences Laboratory, University of California, Berkeley, California 94720-7450, USA
†Present address: Department of Physics, Purdue University, West Lafayette, Indiana 47907-1396, USA
‡Present address: Laboratory for Earthquake Chemistry, Graduate School of Science, University of Tokyo, Tokyo 113-0033, Japan
*Correspondence author's e-mail address: kuni@ssl.berkeley.edu

(Received 2000 December 19; accepted in revised form 2002 August 5)

Abstract–Cosmic-ray-produced (cosmogenic) nuclides were studied in fragments of the Brenham pallasite, a large stony iron meteorite. The contents of light noble gases (He, Ne, and Ar) and long-lived radionuclides (^{10}Be, ^{26}Al, ^{36}Cl, and ^{53}Mn), produced by nuclear reactions with cosmic rays, were measured in the separated metal and olivine phases from numerous samples representing a wide range of shielding conditions in the meteoroid. The distribution of cosmogenic nuclide concentrations in the metal follows patterns similar to that observed in large iron meteorites. Shielding effects were estimated from the relative proportions of low- and high-energy reaction products. The production rates varied, from surface to interior, by a factor of more than several hundred. The ^{36}Cl-^{36}Ar cosmic-ray exposure age of Brenham is 156 ± 8 Myr. This determination is based on a multiple nuclide approach that utilizes cosmogenic nuclide pairs. This approach not only yields a "shielding independent" exposure age but also demonstrates that the production of cosmogenic nuclides occurred in a single stage. The depth profiles of ^{10}Be in the stone phase and ^{53}Mn in the metal phase are shown superimposed on corresponding profiles from the Apollo 15 long drill core.

Surprisingly low abundances of lithophile elements, such as K, U, and Th, provided a unique opportunity to examine the production systematics of those nuclides whose inventories typically have significant contributions from non-cosmogenic sources, particularly radiogenic contributions. The U and Th contents of the olivine samples are extremely low, allowing detection of cosmogenic ^{4}He production from oxygen, magnesium, silicon, and iron.

INTRODUCTION

Although cosmic-ray-produced (cosmogenic) nuclides have been studied in extra-terrestrial materials for more than 40 years, there are instances in which the measured concentrations of cosmogenic nuclides in a meteorite are not consistent with theoretical predictions. This circumstance most likely is the result of a combination of several problems: in many instances the concentration of a cosmogenic nuclide is low enough to generate measurement uncertainty; the cross-sections for some of the reactions are unknown or uncertain; and the transport codes for both charged particles and neutrons in some instances have not accurately incorporated the complexity of meteoroid exposure to energetic particles (cf., Reedy *et al.*, 1983). Some of these issues can be investigated because of the improved detection sensitivity of both stable and radionuclides, advances in thick target model experiments, and improved Monte Carlo calculation techniques (cf., Masarik and Reedy, 1994; Michel *et al.*, 1991). In this paper, we present our studies on Brenham, a large pallasite, found in 1882 in Haviland, Kiowa County, Kansas, USA (Nininger, 1952). The metallic fraction of this meteorite has also been identified as "Hopewell Mounds", a medium octahedrite, IIIA, with olivine inclusions, for which prehistoric records exist (Buchwald, 1975).

This work was partially motivated by the earlier works by Eberhardt and Eberhardt (1960, 1961) and Honda *et al.* (1961) whose measurements of noble gases and radionuclides failed to provide a consistent irradiation scenario for this large meteorite. In particular, the noble gas data required a long duration exposure to cosmic rays, whereas the radionuclide activities were below detection limits. This discordance can be explained by either a multi-stage exposure or a long terrestrial age. Measurements of radionuclides, in particular ^{14}C, will yield the terrestrial age. Measurements of radionuclides having

Prelude preprint MS#4484

a range of half-lives will also constrain the exposure geometry of the Brenham meteoroid. An additional motivation for the measurements described herein is that to date most measurements have been focused only on the stone phase (cf., Nishiizumi, 1987; Schultz and Kruse, 1989 and suppl. by Schultz and Franke, pers. comm. (2000)). Cosmogenic nuclide measurements from both the silicates and metal phases, which exist side-by-side within pallasites, offer an opportunity to characterize the effects of shielding and target chemistry on cosmogenic nuclide production. Brenham is thus an ideal specimen for extending our knowledge of the physics of those high-energy reactions that produce cosmogenic nuclides.

Our goal in this study is to determine the production parameters for a "semi-empirical" model of cosmogenic nuclide production (Honda, 1988); this approach is fundamentally distinct from Monte Carlo techniques. Monte Carlo techniques are employed to model the production of cosmogenic nuclides for a variety of exposure scenarios involving different target chemistries and shielding conditions. A starting point for all transport codes, including those employing Monte Carlo techniques, is the incident particle flux, the incident particle energy distribution, and the distribution of target nuclei embedded within a matrix. Necessary requirements for the successful modeling of cosmogenic nuclide production is an accurate representation by the transport code of the distribution of target nuclei within the irradiated body and accurate knowledge of production cross-sections. It is in this regard that pallasites represent a yet unsolved challenge for Monte Carlo techniques. Not only is the distribution of targets inhomogeneous, but also the matrix of the entire body is inhomogeneous on millimeter scales. Finally, some constituents of Brenham are heavily shielded and since some of the cross-sections for the production pathways at these shielding values are uncertain, this in turn results in uncertainty in the entire calculation. The pallasite Brenham is the ideal sample for determining the production parameters of a semi-empirical model for cosmogenic nuclide production. This approach has several benefits: the production parameters determined from this study are applicable to other objects, both metal and stone, that have been exposed to cosmic rays under heavy shielding conditions; this work also serves as a ground truth for improving the Monte Carlo codes for cosmogenic nuclide production.

In space, galactic cosmic rays bombard objects of various sizes and compositions producing a cascade of nuclear interactions and particles, the latter dominated by neutrons. The secondary particle flux, depending on the meteoroid size and specific nuclear reactions, dominates production of cosmogenic nuclides in the region below the surface of the meteoroid. Both primary and secondary particles interact with the target nuclei, which in meteoroids are predominantly those of the rock-forming elements—O, Mg, Al, Si, S, Ca, and the first row transition metals.

The realization of our goal requires independent determination of production profiles of cosmogenic nuclides from the metal and silicate phases. Because it is easy to separate metal and silicate in Brenham, we separately examine cosmogenic nuclide production in metal and silicate. These production profiles from the silicate and metal phases can then be compared to those from stone and iron meteorites, respectively.

EXPERIMENTAL

Sample Description

The meteorite fragments used in this study were obtained from various sources; the locations within the meteoroid ranged from deep in the interior to those near the surface. The sources of the samples used in this study are listed in Table 1.

The olivine crystals in Brenham are typically 5 mm in diameter and are easily identified based on their dark green to amber hue. The interstitial veins consist primarily of mixtures of sulfides and chromites; minor constituents include minerals showing varying degrees of weathering components, as evidenced by the presence of oxides and chlorides. The densities of the samples Ward 10.50 and 10.54 is 4.9–5.0 g/cm^3; these samples are described in Honda *et al.* (1961). The presence of silicates either adhering to or incorporated within the metal phases represents a source of cosmogenic nuclides not produced directly from Fe or Ni. Since the production rates for many cosmogenic nuclides from Fe and Ni are substantially less than the corresponding rate in silicates, it is essential that this source of cosmogenic nuclides be minimized. Fortuitously, the metal fraction separated from Brenham is extremely pure, possessing little silicate contamination.

Sample Preparation

The metal and stone (olivine) phases were physically separated from each other at Tokyo (Nihon University). In

TABLE 1. Sources of Brenham samples.

Sample ID	Source	Date
N91	D. New	1991
N94	D. New	1994
UCSD86	Arizona State University	1964
AMNH880	American Museum of Natural History	1995
AMNH881	American Museum of Natural History	1995
		1996
Reed 1	B. Reed	1991
Reed 2	B. Reed	1991
Reed 3	B. Reed	1991
Reed 4	B. Reed	1991
HJ91	American Meteorite Laboratory	1991
H49.236	American Meteorite Laboratory	1987
Ward LJS	Ward's Nat. Sci. Est. Inc (Ward 10.50)	1958
Ward 10.50	Ward's Nat. Sci. Est. Inc	1958
Ward 10.54	Ward's Nat. Sci. Est. Inc	1958

general, it was possible to isolate clean phases using dental tools followed by further purification using a hand magnet. This procedure failed to produce a pure specimen for the severely weathered Ward LJS samples; the presence of magnetite prevented a clean separation of phases. At this stage of the separation, the stone phase contains sulfides, oxidized iron due to weathering, carbon compounds, and fine black suspensions. The metal phase contains traces of sulfides, oxidized iron, and silicates. The metal and stone phases were extensively cleaned by chemical etching before dissolution.

The silicate phases (*i.e.*, olivine crystals) were etched either by a 6N HCl (Nihon University, Tokyo) or a 4N HNO_3 (University of California, Berkeley (UCB)) solution in an ultrasonic bath. The etching step was performed 2 or 3 times. After crushing the olivine crystals into finer grains, the magnetic impurities were removed by a hand magnet. Some loss of silicates was observed after strong etching treatments. The cleaned olivine is pale green. To further purify the metal phase any exposed surface that was oxidized was scraped using a dental tool. The metal phase was etched with a 2N HCl + H_2O_2 solution followed by 49% HF treatment.

Radionuclide measurements require additional chemical separation procedures; the procedures used at UCB are summarized below. The procedures employed at Tokyo are generally similar to those used at UCB but the Tokyo procedures did not involve Cl separation. The stone fraction was dissolved with an HF/HNO_3 mixture along with Be, Al, and Cl carriers. The metallic fraction was dissolved with 4N HNO_3, along with Be, Al, Cl, and Mn carriers. Small amounts of insoluble materials, such as carbon, schreibersite, and silicates, were removed from the solution by filtration. Aliquots of the solution were used for chemical analysis by atomic absorption spectroscopy (AAS). Mg, Ca, Mn, and Fe were measured in stone fractions. Mg, Fe, Co, and Ni were measured in metal fractions. Be, Al, Cl, and Mn were separated and purified from both fractions by a combination of anion exchange, cation exchange, solvent extraction, and hydroxide precipitation (*e.g.*, Imamura *et al.*, 1973; Nishiizumi *et al.*, 1984b,c).

In general, the abundances of the major elements from the fragments analyzed in this work are relatively constant, with those exceptions noted below. The stone phase consists of forsteritic olivine (Mg: 28%, Fo = 0.87) (Scott, 1977). The cleaned olivine phase contains minor lithophile elements, such as Na, Al, Ca, and Mn. In addition to the measurements performed by AAS, a suite of elements in various olivine fractions was measured using neutron activation. These results of N94 are shown in Table 2 as example, in addition to the concentrations of U and Th inferred from He measurements.

TABLE 2. Chemical composition of Brenham N94 stone.

Element	Concentration
Na	80 ppm
Mg	28%
Al	110 ppm*
S	<1%
Cl	<2 ppm
K	<0.01 ppm†
Ca	40 ppm
Sc	1 ppm
Cr	150 ppm
Mn	1750 ppm
Fe	10%
Co	6 ppm
Ni	170 ppm
Cu	140 ppm
As	0.04 ppm
U, Th	$<1 \times 10^{-6}$ ppm‡

*Nagai *et al.* (1993).
†Estimated from radiogenic Ar, and directly measured by neutron activation analysis (Ebihara, pers. comm.; Table 7).
‡Estimated from ^{4}He concentration.

Measurements of Cosmogenic Nuclides

Cosmogenic noble gases were measured using a VG5400 mass spectrometer (Nagao, 1994a). To reduce adsorbed atmospheric noble gases the metallic and silicate samples were heated overnight at 200 and 150 °C, respectively. Noble gases residing within metal phases were liberated by vaporizing the metal at 1950 °C in an alumina crucible. Noble gases in the silicate phases were extracted by heating them to 1800 °C in a Mo crucible. Procedural blanks for the alumina crucible are 1×10^{-9} for ^{4}He, 5×10^{-11} for ^{20}Ne, 3×10^{-8} cm^3 for ^{40}Ar, and typically 1×10^{-13} cm^3 for ^{84}Kr and ^{132}Xe, respectively. Blanks for the Mo crucible are about an order of magnitude lower than those for the alumina crucible. These blanks are low and thereby allow the measurement of cosmogenic light noble gases in 1 g size samples even from the most heavily shielded fragment. Stepwise heating runs were also performed on the stone phases of samples UCSD86 and Ward 10.50.

The cosmogenic radionuclides ^{10}Be ($t_{1/2}$ = 1.5 Myr), ^{26}Al (0.705 Myr), and ^{36}Cl (0.301 Myr) in the metal and the stone phases were measured by accelerator mass spectrometry (AMS). The measurements of ^{10}Be and ^{26}Al for Tokyo samples were performed by the AMS system at the University of Tokyo (Kobayashi *et al.*, 1997). The measurements of ^{10}Be, ^{26}Al, and ^{36}Cl for UCB samples were done at the Center for Accelerator Mass Spectrometry (CAMS) at Lawrence Livermore National Laboratory (LLNL) (Davis *et al.*, 1990).

The ^{53}Mn ($t_{1/2}$ = 3.7 Myr) measurements in the metal phases were done by neutron activation through the ^{53}Mn(n,γ)^{54}Mn reaction (Millard, 1965) in Tokyo. The neutron irradiation was performed in the well-thermalized flux area of the JRR3 reactor at the Japan Atomic Energy Institute, Tokai, Japan. After radiochemical separation, the characteristic 834.8 keV γ-ray from ^{54}Mn was measured using a Ge detector. The standard

for the ^{53}Mn measurements is extracted from the Grant meteorite and calibrated by x-ray counting. This standard was used for the calibration of "Bogou ^{53}Mn standard" that has been used since 1977.

RESULTS

The production rates of ^{21}Ne and ^{26}Al in the stone phase are a factor of 30–100 higher than those in metal phase; it is accordingly essential to remove all silicates from the metal phase. In order to check for silicate contamination of the metal samples, the Mg concentration was measured in the HNO_3 solution after metal dissolution. After the chemical etching procedure used at UCB, the content of the dissolved Mg in the solutions is <2 μg/g metal for all metal samples, excepting one fraction of N94. The dissolved stone in the metal fractions is <7 μg/g metal, using an abundance of Mg in olivine of 28%. The fraction of silicate material in the dissolved metal fraction is $<10^{-5}$. Therefore, the ^{26}Al in the metal phase derived from the silicate phase is negligible for all the metal samples separated at UCB.

The light cosmogenic noble gases are produced more readily in silicates than in metal. For this reason, the reconstruction of the amount of cosmogenic noble gas produced exclusively in the metal phase requires the subtraction of those cosmogenic noble gases produced in the silicate phase. A prerequisite for this subtraction is knowledge of the level of silicate contamination in the metal phase. To estimate the silicate contamination, we use the chemical analysis measurements from those samples in which the radionuclides were measured. Specifically, the stone contamination is represented by the sum of the dissolved silicates in the metal phase, as measured by atomic absorption spectrometry at Tokyo, and the insoluble materials remaining after dissolution of the metal. These results are shown in Table 3. In general, silicate contamination is $<10^{-4}$, except one sample of N94, and does not pose any significant problem for cosmogenic Ne and other noble gas determinations.

The noble gas data for the silicate phases are shown in Table 4. All silicate phase data for both noble gases and radionuclides are expressed with a suffix "s" (*e.g.*, $^{3}He_s$ for the ^{3}He content in the silicate phase). Selected literature data are tabulated with those of this work for comparison. The ^{3}He/^{4}He ratios suggest production entirely *via* cosmogenic means. The single exception is the first run on Ward 10.50 sample, which most likely incorporated mass spectrometric memory of radiogenic ^{4}He from previous analyses. Similarly, some radiogenic ^{40}Ar is present in the same sample. The relatively high ^{20}Ne/^{22}Ne ratios in the Ward samples are also attributable to memory in the mass spectrometer. Nagao (1994b) and Miura (1995) measured the heavy noble gases in Brenham and more recently Mathew and Begemann (1997) measured the trapped noble gases in the olivine phase.

The noble gas data for the metal phase (Nagao *et al.*, 1996) are shown in Table 5. All metal phase data for both noble gases and radionuclides are expressed with a suffix "m". Although some contamination from atmospheric noble gases was detected for both Ne and Ar, the cosmogenic contributions can be evaluated without difficulty. Contamination is most visible in AMNH881, Ward 10.50, and Ward LJS samples. An extremely high ^{40}Ar concentration (net 260×10^{-8} cm^3 STP/g) was observed in the metal phase from sample AMNH881. The isotopic composition resembles atmospheric Ar, but the ratio of Ar to Ne is 10× higher than that of air. These observations were confirmed with duplicate runs. The Ar seems to be a trapped component of unknown origin. Anomalously high Ar/Ne has not been found in other samples.

Radionuclide data for the metal and stone phases are shown in Table 6. In Table 6, the designation "Tokyo" indicates that the chemical separation for Mn, Be, and Al were performed at Nihon University in Tokyo and the AMS measurements were performed at University of Tokyo. Analogously, "UCB-LLNL" indicates that the chemical separations for Be, Al, and Cl were performed at UCB and the AMS measurements were performed at CAMS-LLNL. The ICN (ICN Biomedical, Inc.) ^{10}Be, NBS (National Bureau of Standards—present NIST, National Institute of Standards and Technology) ^{26}Al, and NBS ^{36}Cl standards were diluted by one of the authors (Nishiizumi), and are used for normalization of the AMS measurement. After making background (due to ^{10}B for ^{10}Be measurements) and blank corrections (3×10^{-14} or 6×10^{-15} for ^{10}Be/Be, 1×10^{-14} for ^{26}Al/Al, and 2.5×10^{-14} for ^{36}Cl/Cl—LLNL), the measured ratios were converted to activities (dpm/kg sample). Since most of the ^{10}Be and the ^{26}Al measurements in the stone fractions performed at Tokyo were not done on cleaned samples, and the data were not reproducible, we have only adopted the values measured by UCB-LLNL in this work. Our findings indicate that the ^{10}Be and ^{26}Al results for Brenham measured by Nagai *et al.* (1993) incorporate ^{10}Be and ^{26}Al derived from silicate contamination within the metal phase. It is possible that the noble gas results in this work, particularly the cosmogenic Ne concentrations, suffer from the same problem since these samples were not extensively cleaned. Although the major elemental compositions of each olivine fraction were relatively

TABLE 3. Stone contamination found in metal phases.

Sample	Mass (g)	Mg (μg in solution)	Mg (μg in residue)	Stone (μg/g metal)
N94	0.20	6.1	95	1800
AMNH880	0.93	–	1.5 ± 0.6*	6 ± 2
Reed 1	1.30	–	33 ± 7*	90 ± 20
Reed 2	0.20	0.5	1.8	40
H49.236	0.89	–	91 ± 17*	370 ± 70
Ward LJS	0.40	0.6	0.8	13
Ward 10.50	0.20	0.6	2	50

*Measured by neutron activation analysis. The stone contents in metal fractions are not necessarily representative of whole fragments.

TABLE 4. Light noble gases found in stone phases of Brenham.

	Measured									Cosmogenic		
Sample	^4He_s	$(^3He/^4He)_s$	$^{20}Ne_s$	$(^{20}Ne/^{22}Ne)_s$	$(^{21}Ne/^{22}Ne)_s$	$^{36}Ar_s$	$^{40}Ar_s$	$(^{38}Ar/^{36}Ar)_s$	$(^{40}Ar/^{36}Ar)_s$	^3He_s	$^{21}Ne_s$	$^{38}Ar_s$
N94	622	0.1656(10)	24.8	0.858(3)	1.024(6)	0.236	14.4	1.311(2)	60.94(3)	103	29.6	0.302
N91	491	0.1582(14)	21.9	0.860(1)	1.014(8)	0.354	16.0	1.390(2)	45.22(6)	77.7	25.8	0.485†
UCSD86	441	0.1488	21.5	0.857	1.017	0.160	14.1	1.181	88.10	65.6	25.5	0.182
AMNH880	110	0.1376(4)	6.66	0.856(1)	1.006(7)	0.0484	7.29	0.927(1)	150.65(8)	15.1	7.83	0.0408
Reed 1	73.8	0.1466(9)	3.18	0.848(2)	0.994(6)	0.115	16.9	0.938(2)	147.58(9)	10.8	3.73	0.0984
Reed 2	90.1	0.1439(10)	4.09	0.848(2)	1.001(6)	0.0668	9.47	0.971(1)	141.73(11)	13.0	4.83	0.0597
Reed 3	69.5	0.1466(8)	2.70	0.846(1)	0.991(6)	0.0989	13.1	1.010(2)	132.45(6)	10.2	3.16	0.0927
Reed 4	74.4	0.1466(8)	2.76	0.849(1)	1.001(6)	0.0582	7.73	1.014(2)	132.73(10)	10.9	3.25	0.0548
HJ.91	67.3	0.1403(7)	3.58	0.855(1)	1.000(8)	0.0594	11.0	0.721(1)	184.54(3)	9.44	4.19	0.0361
H49.236-1	35.8	0.1352(7)	1.50	0.857(1)	1.004(8)	0.0422	10.5	0.434(1)	248.08(3)	4.84	1.76	0.0118
H49.236-2	31.4	0.1379(8)	1.11	0.860(1)	1.003(7)	0.0574	14.5	0.404(1)	252.77(5)	4.33	1.30	0.0142
AMNH881	3.43	0.1276(6)	0.197	0.871(2)	0.995(7)	0.0243	7.05	0.2229(4)	290.12(2)	0.44	0.23	0.00097
Ward LJS	1.97	0.1184(4)	0.148	1.247(2)	0.964(7)	0.325	96.0	0.1913(3)	295.18(2)	0.23	0.11	0.0012
Ward 10.50	3.74*	0.0856(4)	0.261	0.935(2)	1.003(8)	0.125	40.9*	0.2063(3)	328.3(2)	0.32	0.28	0.0026
Ward 10.50	2.25	0.1274(9)	0.123	0.969(4)	0.999(3)	0.0714	21.1	0.1992(5)	295.51(2)	0.29	0.13	0.0009
Ward 10.50	2.17	0.1059(9)	0.100	1.486(7)	0.866(3)	0.132	39.3	0.1919(6)	297.48(2)	0.23	0.058	0.0006
A	665	0.159	34.4	0.940	0.997	0.80	100	1.07	133	106	36.5	–
B	33.5	0.135	1.70	0.872	1.01	0.0210	4.23	0.667	201	4.59	1.97	–
C	68.7	0.109	3.25	0.992	1.006	0.052	9.8	0.693	189	7.50	3.30	–

The concentrations are given in the unit of 10^{-8} cm^3 STP/g. 1σ errors for isotopic compositions in last digit(s) are shown in parentheses.
Abbreviations: A = Eberhardt and Eberhardt (1960, 1961); B = Miura (1995), source H49.236; C = Mathew and Begemann (1997).
*Contamination of natural radioactivities and argon from air.
†High ^{38}Ar probably due to higher Fe content.

TABLE 5. Light noble gases found in metal phases of Brenham.

	Measured								Cosmogenic			
Sample	$^{4}He_m$	$(^{3}He/^{4}He)_m$	$^{20}Ne_m$	$(^{20}Ne/^{22}Ne)_m$	$(^{21}Ne/^{22}Ne)_m$	$^{40}Ar_m$	$(^{38}Ar/^{36}Ar)_m$	$(^{40}Ar/^{36}Ar)_m$	$^{21}Ne_m$	$^{38}Ar_m$	$(^{38}Ar/^{36}Ar)_m$	$(^{3}He/^{38}Ar)_m$
N94	216	0.2686(7)	0.762	0.875(2)	0.930(7)	12.4	1.571(2)	5.430(3)	0.785	3.57	1.596(3)	16.2
N91	173	0.2603(10)	0.542	0.910(4)	0.935(7)	15.1	1.565(2)	8.500(4)	0.540	2.78	1.606(3)	16.4
AMNH880	30.1	0.2404(8)	0.126	1.472(3)	0.865(6)	34.6	1.175(2)	98.88(5)	0.071	0.394	1.670(3)	18.4
Reed 2	25.5	0.2385(9)	0.0812	1.198(1)	0.891(6)	12.4	1.426(9)	50.70(1)	0.059	0.346	1.682(1)	17.5
H.J91	18.8	0.2210(6)	0.131	2.595(6)	0.751(5)	44.1	0.913(1)	151.50(7)	0.036	0.241	1.673(3)	17.2
H49.236-1	12.0	0.2409(11)	0.0489	1.400(3)	0.876(6)	13.1	1.219(2)	89.13(4)	0.029	0.173	1.710(2)	16.7
H49.236-2	9.97	0.2354(10)	0.0613	2.132(4)	0.798(6)	19.3	1.026(1)	130.88(4)	0.022	0.140	1.690(2)	16.8
AMNH881	1.09*	0.188(4)	0.0676	7.88(2)	0.215(3)	260†	0.1984(3)	289.47(9)	0.0016	0.0107	1.750(23)	19.2
Ward LJS	0.812*	0.218(5)	0.028	6.33(1)	0.372(5)	14.6	0.3508(4)	264.80(11)	0.0015	0.0102	1.733(7)	17.4
Ward 10.50	0.630*	0.202(7)	0.034	7.57(2)	0.242(3)	15.2	0.2981(3)	275.29(6)	0.0010	0.0070	1.762(7)	18.1

The concentrations are given in the unit of 10^{-8} cm^3 STP/g. 1σ errors for isotopic compositions in last digit(s) are shown in parentheses.
*Blanks in the measured $^{4}He_m$ of AMNH881 and Ward are estimated to be ~10%.
†A large amount of trapped Ar is observed. Ar/Ne ratio is ~10× higher than that of the terrestrial atmosphere.

TABLE 6. Cosmogenic radionuclides measured in Brenham.

Sample name	Metal						Stone		
	$^{53}Mn_m$ Tokyo	$^{10}Be_m$ UCB-LLNL	$^{10}Be_m$ Tokyo	$^{26}Al_m$ UCB-LLNL	$^{26}Al_m$ Tokyo	$^{36}Cl_m$ UCB-LLNL	$^{10}Be_s$ UCB-LLNL	$^{26}Al_s$ UCB-LLNL	$^{36}Cl_s$ UCB-LLNL
N94	166 (7)	1.101 (22)	0.93 (3)	0.77 (3)	0.86 (5)	5.71 (10)	9.05 (14)	19.9 (5)	0.716 (23)
N91	122 (4)	0.910 (12)	0.57 (2)	0.638 (18)	0.62 (4)	4.91 (5)	7.70 (14)	18.1 (5)	0.453 (9)
UCSD86	98 (4)	–	–	–	–	–	–	–	–
AMNH880	26 (1)	0.1023 (25)	0.085 (5)	0.076 (4)	0.050 (8)	0.615 (7)	1.40 (2)	3.11 (9)	0.059 (3)
Reed 1	–	–	0.13 (6)	–	0.069 (10)	–	1.02 (2)	2.94 (7)	0.103 (6)
Reed 2	26 (1)	0.0992 (18)	0.095 (11)	0.069 (3)	–	0.581 (6)	1.29 (3)	2.68 (8)	0.051 (3)
Reed 3	21 (1)	0.0870 (15)	0.093 (5)	0.063 (3)	0.056 (10)	0.521 (6)	1.05 (3)	2.59 (7)	0.089 (4)
Reed 4	–	0.0963 (19)	0.10 (5)	0.070 (4)	0.055 (16)	0.559 (8)	1.19 (2)	2.60 (6)	0.054 (3)
HJ91	17 (1)	0.0656 (24)	0.065 (5)	0.045 (3)	0.047 (5)	0.384 (9)	0.848 (16)	2.18 (5)	0.030 (3)
H49.236	8.5 (5)	0.0393 (16)	–	0.0327 (14)	–	0.228 (4)	0.542 (10)	1.23 (3)	0.040 (2)
AMNH881	2.3 (6)	0.00236 (15)	0.006 (2)	0.0017 (3)	0.003 (3)	0.0200 (11)	0.0899 (16)	0.185 (8)	0.0045 (7)
Ward LJS	1.0 (2)	0.00234 (11)	0.0012 (3)	0.0022 (5)	0.001 (1)	0.0144 (5)	0.0533 (16)	0.125 (5)	0.0062 (25)
Ward 10.50	0.81 (5)*	–	–	–	–	0.017 (1)*	0.0412 (10)	0.084 (4)	0.0112 (10)
Ward 10.54	–	–	–	–	–	–	0.0359 (10)	0.080 (4)	0.0096 (9)

1σ errors in last digit(s) are shown in parentheses.
Abbreviations: m = metal phase (dpm/kg metal); s = stone phase (olivine) (dpm/kg stone); UCB-LLNL = University of California, Berkeley-Lawrence Livermore National Laboratory.
*Nishiizumi *et al.* (1984a).

constant, some irregularities were observed among UCB samples. Mg concentrations of Reed 1 and 3 olivines were ~15% lower than those of other olivine fractions. On the other hand, Fe concentrations of Reed 1 and 3 were 70–80% higher than others. A similar but smaller trend was also observed for Word 10.50 and 10.54 olivines. Slightly lower ^{10}Be concentrations in Reed 1 and 3 compared to those in Reed 2 and 4 were reflected in depletion of Mg, which is target element of ^{10}Be production. Higher ^{36}Cl concentrations in Reed 1 and 3 were due to the higher concentrations of Fe, which is target element of ^{36}Cl production. Previous results of ^{53}Mn and ^{36}Cl in Ward 10.50 are also listed in Table 6 (Nishiizumi *et al.*, 1984a).

Cosmogenic ^{14}C in the stone phase of N94 was extracted and measured at University of Arizona NSF-AMS facility. The ^{14}C concentration was 2.45 ± 0.25 dpm/kg. The model terrestrial age of Brenham is 20 ± 2 kyr, assuming the production rate ratio of ^{14}C to ^{10}Be in stone phase is 3. The terrestrial age corrected ^{36}Cl and ^{10}Be results in Brenham were used for calibration of the ^{10}Be-^{36}Cl/^{10}Be terrestrial age method (Nishiizumi *et al.*, 1997a).

DISCUSSION

General Systematics for Cosmogenic Nuclide Productions

As an introduction it is worth considering the ingredients needed to produce production rates. The starting point is the incident particle flux at the location of a particular target; this particle flux is dependent on bulk chemistry and shielding, so an index of shielding is also needed. Every target–product pair has a different likelihood of occurring so a parameter encapsulating this probability is needed. All that remains is the mathematical relationship between these quantities. This relationship is given in terms of a simple parameterized model (Geiss *et al.*, 1962; Stauffer and Honda, 1962). In this model the production rate of a cosmogenic nuclide is governed by the following equation:

$$P(\mathrm{A},\mathrm{Z}) = f(\mathrm{A},\mathrm{Z}) \times k_1 \times (\Delta \mathrm{A})^{-k_2} \quad (1)$$

P(A,Z) is the production rate of a specific nuclide, in atom/min g produced from a specific target nuclide and is a function of the following quantities. ΔA is a term related to the mass difference between the target and product nuclides. In some instances this quantity is simply the difference between masses; for other reactions it is determined empirically. In essence, this empirical term incorporates the "nuclear physics" of the reaction, indicating how likely this reaction is. In many reactions, more than one nuclide is produced at a given mass; f(A, Z) represents that fraction of the products having mass at A, but also atomic number Z (*i.e.*, the isobaric yield). Embedded in these empirical parameters is specific information related to production rates such as cross-section and excitation functions. These parameters may vary as a function of shielding since production rates are sensitive to incident particle energy and reaction thresholds. The parameter k_1, atom/min g, is proportional to the high-energy particle flux intensity. Factors affecting the particle intensity at any location in the sample are bulk chemistry and shielding. The parameter k_2 is called the shielding index and is directly related to the shielding conditions. Ideally, these parameters are independent of the product–target pair under consideration and ultimately the goal of the development of the approach is the determination of production parameters that can be applied to numerous cosmogenic nuclides. However, at this stage of development in this model it is not always the case that these parameters are unique to all product–target pairs. A specific example of this will be discussed later in this work. Before we apply this model to the measurements of cosmogenic nuclides in Brenham we will discuss in general terms the application of this model to a variety of product–target pairs. In some instances we will use literature data to illustrate specific production pathways.

Production of Cosmogenic Nuclides in Iron Targets

A straightforward example is the production of ^{38}Ar in metal; the production rate can be expressed as

$$P\left(^{38}\mathrm{Ar}\right)_{\mathrm{m}} = k_1 \times (18)^{-k_2} \quad (2)$$

$P(^{38}\mathrm{Ar})_{\mathrm{m}}$ is production rate of ^{38}Ar in an iron target and can be calculated if k_1 and k_2 are known. In this particular instance, f(A,Z) = 1, because all nuclides produced at mass 38 decay to ^{38}Ar. ΔA is the difference between the atomic mass of Fe, 56, and mass 38, the atomic mass of this isotope of Ar.

This model can be extended to smaller ΔA products as well: a typical example is the production of ^{53}Mn and ^{53}Cr from Fe (Imamura *et al.*, 1980). The production for this reaction is

$$P(\mathrm{A},\mathrm{Z}) = f(\mathrm{A},\mathrm{Z}) \times k_1' \times (\Delta \mathrm{A} + \alpha)^{-k_2'} = f \times k_1' \times (\Delta \mathrm{A}')^{-k_2'} \quad (3)$$

where α is an empirical correction term. According to Imamura *et al.* (1980), the α is constant to 4. This equation is used for all products ranging from A = 53 to 20 (or ΔA' = 7 to 40). While this modification may seem "ad hoc" it is important to stress that at this stage in the development of this particular "semi-empirical" approach the lack of data hinders a more rigorous determination of these parameters. When adjustments in the parameters are appropriate we have traditionally termed these altered parameters as k_1' and k_2'. Our goal in this work is to establish the applicability of our approach to a wide range of shielding conditions for each nuclide, independent of whether one parameter set can be applied to all nuclides. We accept that at this stage of development in this model one set of

parameter may not be applicable to all target–product pairs. Accordingly, to simplify the presentation of the model we will not use the primed notation for any of the parameter pairs. The above Eq. (2) is redefined as

$$P\left({}^{38}\mathrm{Ar}\right)_{\mathrm{m}} = k_1 \times (22)^{-k_2} \quad (4)$$

where k_1 and k_2 are redefined as the old k_1' and k_2', respectively, and 22 = ΔA + 4 or ΔA'. Further development and testing of this model, in conjunction with more data, may allow these parameters to be uniquely determined so as to be applicable for a larger variety of target–product pairs in the future.

Application to Iron Meteorites

As a first application we will consider the production of the He isotopes in iron meteorites; the noble gas data in more than 80 iron meteorites by Voshage and Feldmann (1979) provide an opportunity to demonstrate the utility of our approach. Cosmogenic He and Ne in iron meteorites clearly indicate a linear relationship of the log(^{3}He/^{4}He) or log(^{3}He/^{38}Ar) *vs.* log(^{4}He/^{21}Ne). For the ^{4}He/^{21}Ne ratio in particular, the deviation from linear is less than a few percent throughout the range in ratio of 200–450 (Honda, 1985). One consequence of the measured correlations between these ratios is that the equations governing the production rates for the individual cosmogenic nuclides are related; this relation can be expressed in terms of the parameters we have introduced. Following Honda (1985), the production of both He isotopes can be expressed as,

$$P\left({}^{3}\mathrm{He}\right)_{\mathrm{m}} = 16.7 \times k_1 \times (22)^{-k_2} \quad (5)$$

and

$$P\left({}^{4}\mathrm{He}\right)_{\mathrm{m}} = 18.3 \times k_1 \times (14)^{-k_2} \quad (6)$$

Using this approach, as the shielding varies, only the parameters k_1 and k_2 vary. The other constants in the above expressions remain valid over a wide range of shielding conditions. In summary, the data for iron meteorites can be modeled within the framework of the semi-empirical approach and this framework is valid over a wide range of shielding conditions. The production of the remaining light cosmogenic noble gases likewise validates the utility of our approach. In the iron meteorites, the ^{3}He/^{38}Ar ratios have a nearly constant value of 16.7 ± 0.5 even though the shielding parameter, as given by the ^{4}He/^{21}Ne ratio (to be discussed later), changes between 200 and 450. This can only occur when the parameter, ΔA' for ^{3}He is equivalent to that of ^{38}Ar. In this example the value of this parameter was deduced only using the semi-empirical relationships for the production rates; no knowledge of the specific nuclear cross-sections and reaction thresholds was needed. The specific example of the cosmogenic light noble gases provides considerable confidence in the underpinnings of this model; however, it must be noted that even these empirical relationships have limits and will eventually deviate given exceedingly wide ranges of shielding.

Similar empirical relationships can be deduced for other cosmogenic nuclides. Relative to many other products the production of ^{21}Ne from Fe requires products possessing higher energies and as a consequence, the production profile of this reaction drops steeply as a function of depth. The formula for its production is given by

$$P\left({}^{21}\mathrm{Ne}\right)_{\mathrm{m}} = k_1 \times (39)^{-k_2} \quad (7)$$

If ^{21}Ne is paired with a nuclide whose production is rather insensitive to depth, such as ^{4}He, the ratio of this pair will vary systematically with depth and consequently the pair can be used as a shielding indicator. From Eqs. (6) and (7), we replace one of the parameters with a measured production ratio which is expressed as

$$k_2 = 2.247 \times \log\left({}^{4}\mathrm{He}/{}^{21}\mathrm{Ne}\right)_{\mathrm{m}} - 2.84 \quad (8)$$

The above discussion specifically illustrates the relationship between one of the parameters and a physical quantity, but more generally demonstrates the correspondence between the semi-empirical model and the phenomena associated with cosmogenic nuclide production. The parameter k_2 expressed above is reliable shielding indicator provided the following are true: (1) a single-stage exposure geometry; and (2) a constant cosmic-ray flux.

Production of Cosmogenic Nuclides in Other Targets than Iron

For targets other than iron (*e.g.*, silicates) Honda (1988) demonstrated that their production rate is governed by the relation,

$$P(\mathrm{A,Z}) = f(\mathrm{A,Z}) \times k_1 \times \left(56/\mathrm{A_T}\right)^{1/3} \times F\left(\mathrm{A_T}\right) \times (\Delta\mathrm{A}')^{-k_2} \quad (9)$$

This relation is similar in form to the corresponding relation for the production of cosmogenic nuclides from iron, however, since any given product can be produced *via* a number of pathways additional terms must be incorporated into the production equation. The definition of the terms, P(A,Z), f(A,Z), k_1, k_2, and ΔA' are unaltered. The remaining terms in the equation are defined as follows: A_T = target mass; $F(A_T)$ = fraction of the mass represented by the target A_T in the sample; $(56/A_T)^{1/3}$ = correction factor by relative geometrical cross sections. In general this correction factor only deviates modestly from 1. Physically, this term represents a geometrical cross-section relative to Fe.

An example of this type of reaction is the production of ^{26}Al. The production of ^{26}Al varies as a function of depth, and the depth dependence is different for each specific target nuclei. Accordingly, each target element has its own characteristic value for $\Delta A'$; the values for Fe, S, P, and Si are 34, 10, 9, and 6, respectively. The production of ^{26}Al in troilite and schreibersite in large iron meteorites has been examined (Nagai *et al.*, 1999).

Cosmogenic Nuclides in Brenham

Cosmogenic Helium Production–The cosmogenic He data in Brenham are displayed in Fig. 1 along with He data in more than 80 iron meteorites by Voshage and Feldmann (1979). From best fits to these data, it is possible to derive empirical relationships for the production rates (atom/min g) as functions of the parameters k_1 and k_2:

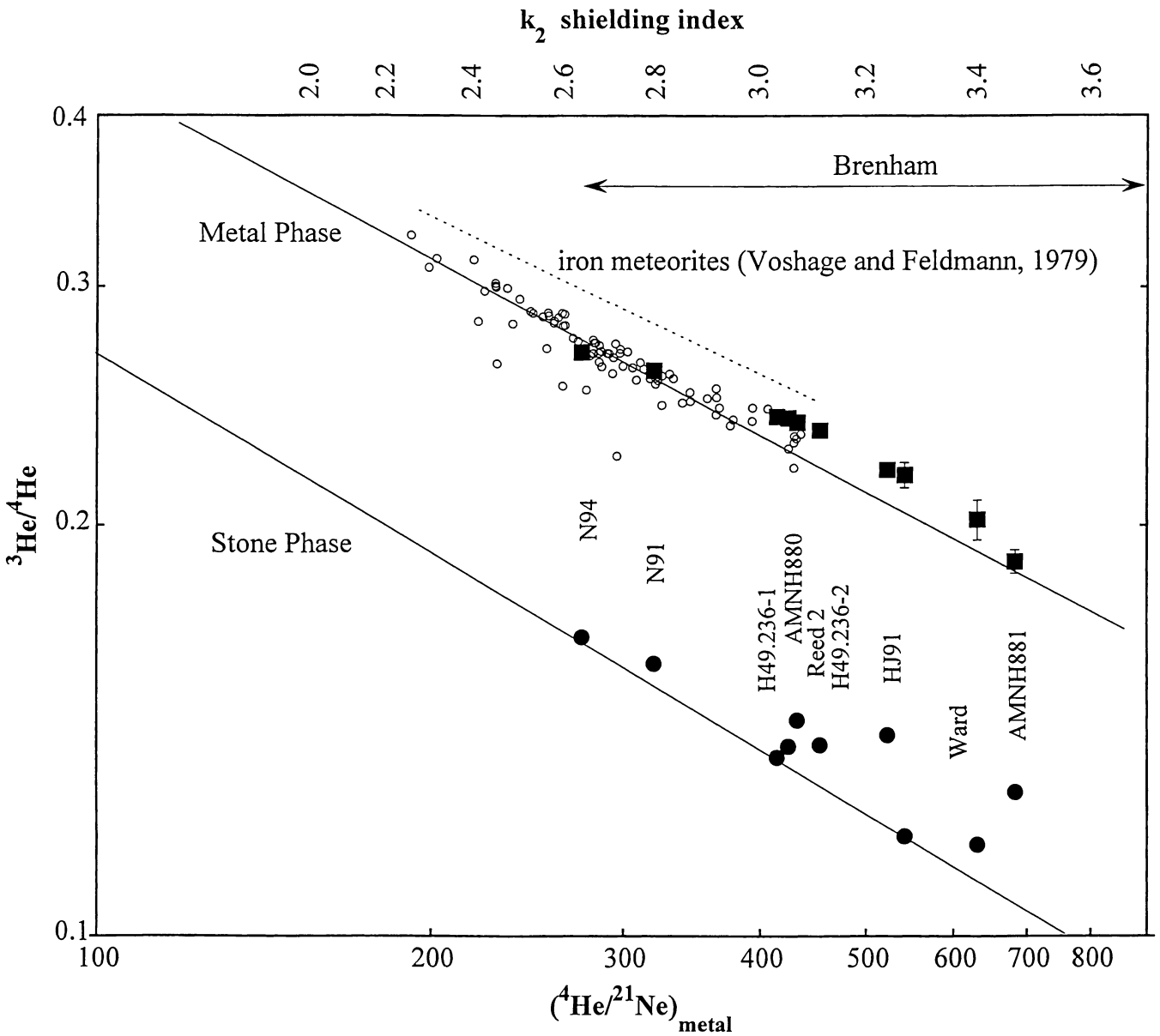

FIG. 1. $^3He/^4He$ ratios in metal and stone phases of Brenham, as functions of $^4He/^{21}Ne$ ratios in metal, the shielding measures of the meteorite samples. The filled squares are data of Brenham metal phases (this work), filled circles are data of Brenham stone (olivine) phases (this work), and open circles are data of iron meteorites by Voshage and Feldmann (1979). Although both relations give essentially straight lines throughout a wide range of $^4He/^{21}Ne$ ratios, 200–800, they trend somewhat upward in extremely heavily shielded regions; this may indicate slightly higher modification factors for ^3He relative to those for ^4He. The similar tendency can also be observed for $^3He/^{38}Ar$ in the metal samples. On the top of the figure, shielding indices k_2, which have been calculated from systematic trends of observed other nuclides data are shown.

$$P\left({}^{3}\mathrm{He}\right)_{m}/\left(16.7\times k_1\times(22)^{-k_2}\right)=1+0.2\times(k_2-2.7)^2 \quad (10)$$

$$P\left({}^{4}\mathrm{He}\right)_{m}/\left(18.3\times k_1\times(14)^{-k_2}\right)=1+0.05\times(k_2-2.8)^2 \quad (11)$$

$$P\left({}^{3}\mathrm{He}\right)_{s}/\left(27\times k_1\times(22)^{-k_2}\right)=1+0.3\times(k_2-2.3)^2 \quad (12)$$

$$P\left({}^{4}\mathrm{He}\right)_{s}/\left(40\times k_1\times(13)^{-k_2}\right)=1+0.2\times(k_2-2.4)^2 \quad (13)$$

These equations differ slightly from those presented earlier, Eqs. (5) and (6), in that the terms on the right-hand side of the equations can deviate slightly from the value 1. Positive deviations from the value 1, as are seen in our data in Fig. 1, correspond to the higher production rates of ^{3}He isotopes at higher shielding condition relative to those of typical spallation products such as ^{38}Ar in metal. The sample Ward is an extreme case, being the most heavily shielded sample, and its deviation is about +20% for ^{3}He in the metal. The above relations are applicable over a wide range of shielding conditions, corresponding to a range of shielding as indicated by the ^{4}He/^{21}Ne ratio of 200–700. Although it is less robust, the last relation for cosmogenic ^{4}He$_c$ in the stone phase is the first empirical relationship between ^{4}He$_c$ production and production parameters derived for stony meteorites. These four equations are nearly independent of the bulk chemical compositions making them especially useful for general comparisons of He production among various extraterrestrial materials having different bulk compositions.

Radiogenic Helium in Stone Phase–Although ^{4}He is produced *via* cosmogenic mechanisms, its production in most chondrites is dominated by the decay of U and Th. The concentration of radiogenic ^{4}He may provide clues about the collisional history of Brenham so an accounting of its inventory is relevant to this work. Figure 1 shows the ^{3}He/^{4}He ratios in the stone and metal phases as a function of the ^{4}He/^{21}Ne ratios in the metal phase. This figure indicates that both ^{3}He and ^{4}He are produced in constant proportion in all Brenham samples, independent of depth; the relationship between the production of the two He isotopes is given by the formula, $^3\mathrm{He} = 0.1142 \times (^4\mathrm{He})^{1.052}$. The correlation of $(^3\mathrm{He}/^4\mathrm{He})_s$ *vs.* $(^4\mathrm{He}/^{21}\mathrm{Ne})_m$ demonstrates the dominance of cosmogenic ^{4}He in even the heaviest shielded sample.

Any ^{4}He present in Brenham that is not cosmogenic can be attributed to radiogenic decay and an upper limit for the radiogenic contribution is estimated to be 0.2×10^{-8} cm^3 STP/g (<10% of ^{4}He in Ward sample) in the stone fraction. This concentration of radiogenic ^{4}He implies a U concentration of $<10^{-12}$ gU/g, substantially lower than the estimates of (1–4) $\times$ 10^{-9} gU/g (and Th) (Morgan and Lovering, 1973). One possible explanation for the low radiogenic ^{4}He concentration is diffusive loss, perhaps driven by shock heating. Relevant to this hypothesis is the data of Voshage and Feldmann (1979), who concluded that among ordinary iron meteorites cosmogenic ^{3}He/^{38}Ar has a relatively constant value of ~16.7. The ^{3}He/^{38}Ar ratios from all the Brenham samples are consistent with this value, indicating no loss of He in the last 156 Myr. The agreement of the ^{4}He-^{53}Mn exposure age with other exposure ages (see below) strengthens the case for no He loss. Our data cannot rule out the possibility of radiogenic ^{4}He loss prior to this time. An alternative possibility is that Brenham has retained its complete radiogenic ^{4}He inventory but the U and Th concentration of Brenham is much lower than previous estimates.

Cosmogenic Neon Isotopes–All three isotopes of Ne are produced in both the stone and metal phases of Brenham (Tables 4 and 5). However, the production of each is dependent on target specific reactions. For example, in the stone phase the production of ^{21}Ne from the ^{24}Mg(n,α) reaction is important in the 10 MeV region, creating a relatively pronounced depth dependency. However, despite the influence of this particular reaction, the ^{22}Ne/^{21}Ne ratio has a value close to 1 for all the shielding conditions observed in the Brenham stone fractions. The constancy of the ^{22}Ne/^{21}Ne ratio in the stone data renders this ratio an ineffective index of shielding. Table 5 shows the cosmogenic ^{21}Ne data from the metal phase. Although the accumulation of cosmogenic ^{21}Ne in the metal phase is well accommodated within the framework of the semi-empirical model its premier utility is realized when it is combined with the cosmogenic ^{4}He and the ^{4}He/^{21}Ne ratio is used as a shielding parameter. This parameter will be discussed in conjunction with other shielding parameters.

Cosmogenic Argon–As is the case for Ne, all three isotopes of Ar are produced *via* cosmic-ray interactions in Brenham. The dominant target for the production of cosmogenic ^{38}Ar is Fe. This target is clearly the dominant one in the metal phase but is also present in Brenham olivine. Since the production systematics of this reaction are independent of the matrix material we would expect a constant ratio for the ^{38}Ar produced in the stone and metal phases. The measured $(^{38}\mathrm{Ar})_s/(^{38}\mathrm{Ar})_m$ ratio is 0.12 ± 0.04 for eight samples except Ward. Variations in this ratio can be accounted for by differences in the Fe concentration of the olivines, which range from 8 to 12%. Like ^{38}Ar, cosmogenic ^{36}Ar is produced from Fe in both the metal and stone fractions. ^{36}Ar can also be produced *via* the reaction ^{35}Cl(n,γ)^{36}Cl; however, the low indigenous Cl abundance in Brenham precludes production of substantial ^{36}Ar. Cl is present in the stone phase but it is a terrestrial contaminant.

In principle, Ca is also a candidate for the production of Ar isotopes; however, the Ca content is <100 ppm in the stone phase. Accordingly, the ^{38}Ar/^{36}Ar ratios in the most shielded fragments would be affected only slightly by the presence of Ca (Begemann *et al.*, 1976). In reality though, the cosmogenic ^{38}Ar/^{36}Ar ratios in the stone phases are essentially equal to those in metals, indicating the minimal effects of production from Ca. More quantitative baseline estimates for cosmogenic ^{36}Cl and ^{36}Ar from Ca can be made using Apollo 15 core data, where the contribution from Ca is predominant (Nishiizumi *et*

al., 1984b). The production formula of ^{36}Cl from Ca is obtained using the empirical relation $\Delta A' = 8.5$ and $f = 0.64$. For ^{38}Ar in Ca, the difference parameter, $\Delta A' = 6$, is used.

While cosmogenic ^{40}Ar is produced in the metal phases its concentration is difficult to measure accurately since atmospheric Ar masks the cosmogenic contribution. The production pathway for ^{40}Ar starts with the production of mass 40 progenitors, the main one being ^{40}K produced by spallation reactions with the target Fe (Honda, 1959). The half-life of ^{40}K is far longer than the exposure age and the main decay product is ^{40}Ca rather than ^{40}Ar. In sum, the consequence of these circumstances is that the measurement of cosmogenic ^{40}Ar cannot be performed as accurately those of ^{40}K, ^{38}Ar, or ^{36}Ar.

The effects of cosmogenic Ar production can be seen in a three-isotope plot (Fig. 2). Specific Ar compositions are the result of the linear superposition of three end-members: cosmogenic, radiogenic, and atmospheric. ^{40}Ar is dominated by atmospheric contamination. The cosmogenic $^{38}Ar/^{36}Ar$ in the metal phase is a function of shielding (Voshage and Feldmann, 1979) and in Brenham this ratio systematically increases with increasing depth. The Brenham measurements indicate the presence of two Ar components, cosmogenic Ar and atmospheric Ar; no radiogenic ^{40}Ar could be discerned.

The relative proportions of cosmogenic and atmospheric ^{36}Ar and ^{40}Ar, as a function of the shielding, were determined for the metal phase. These results are shown in Table 5. These

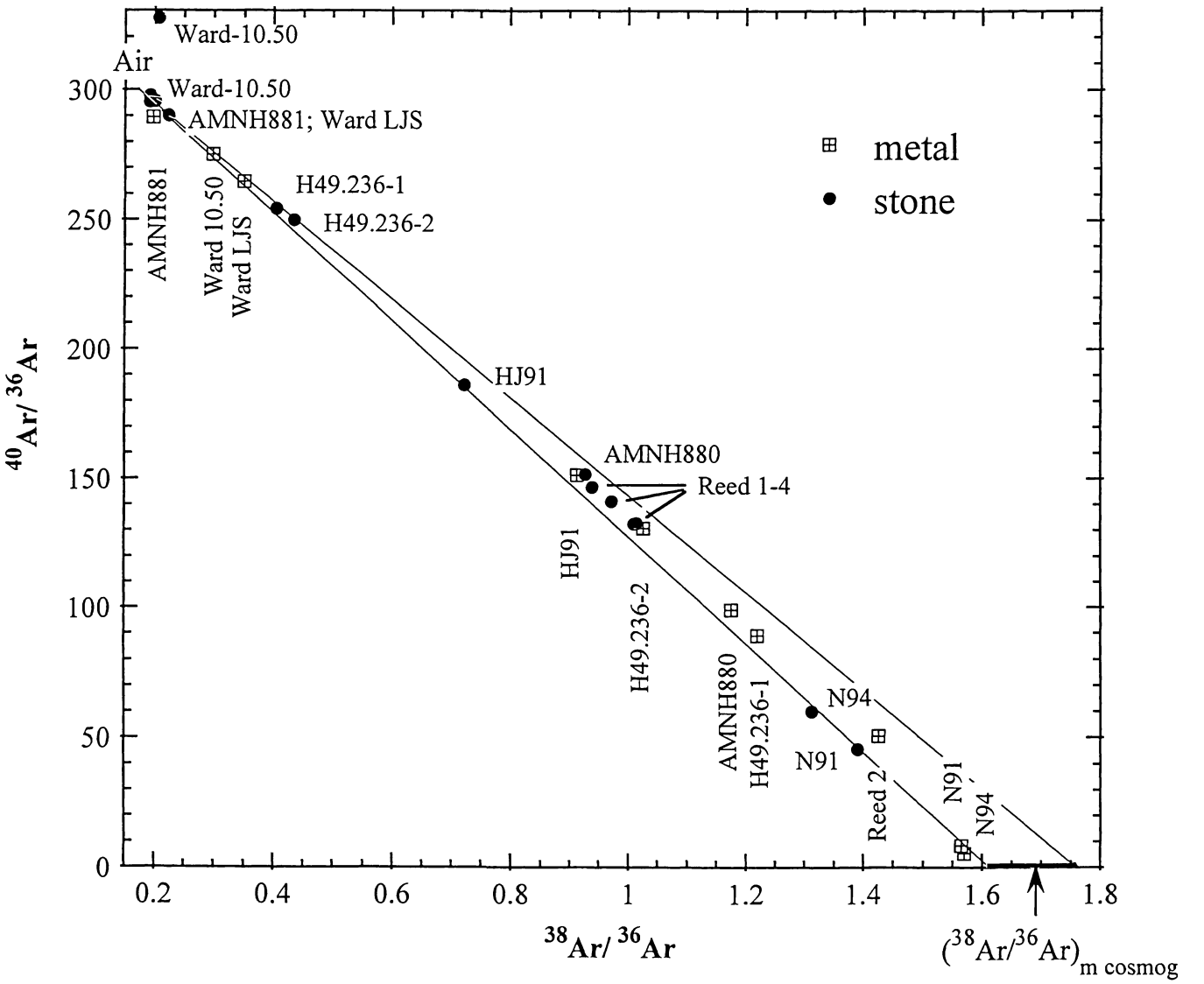

FIG. 2. Relations among Ar isotopes found in Brenham metal and stone phases. The data from stone and metal phases are compared directly. The end-member compositions for the Ar isotopes are atmospheric and cosmogenic Ar. Isotopic ratios for AMNH881-metal (Table 5) were similar to those of air, but the $^{40}Ar/^{36}Ar = 290$, slightly lower than the corresponding ratio for atmospheric Ar. With the exception of this datum and the first run on Ward-10.50 stone, all other compositions are simple mixtures of air and cosmogenic Ar; there is no detectable radiogenic ^{40}Ar contribution, effectively limiting the K concentration to <0.01 ppm in Brenham.

data also exemplify the differences in the $^{38}Ar/^{36}Ar$ ratio between the metal and stone phases. These data, in turn, can be used to determine the non-radiogenic $^{40}Ar/^{36}Ar$ ratio in stone from which the radiogenic contribution to the Ar inventory can be calculated. The details of this calculation are shown in Table 7. For the least shielded fragments, N94 and N91, from which $(^{40}Ar/^{36}Ar)_m$ was measured, the ratio is ~5 or higher. Cosmogenic ^{40}Ar in the metal could contribute a few percent; however, no effect is expected from the samples having more shielding.

The existence of atmospheric Ar is based on the $^{40}Ar/^{36}Ar$ ratio of the end-member composition, essentially that of atmospheric Ar ($^{40}Ar/^{36}Ar = 296$). Additionally, in Ward metal sample by the $^{20}Ne/^{40}Ar$ ratio was $\sim 2 \times 10^{-3}$, suggesting that most of the Ne and Ar are atmospheric contamination in origin. A remarkable feature of these measurements is the lack of radiogenic ^{40}Ar. Taken at face value these indicate extremely low K concentrations (cf., Fig. 2). Our data provide an upper limit of 10 ppb K in the olivine (Table 7). The K concentration in other pallasites can be estimated from the amount of radiogenic ^{40}Ar in the stone phase. In general the K concentration in other pallasites is low: Brahin, Esquel, Imilac, and Mount Vernon have <1 ppm; Marjalahti, Eagle station, Admire and Thiel Mountains have ~1 ppm; and Krasnojarsk and Springwater have ~2 ppm (Megrue, 1968). While these are low they are substantially higher than our estimate for Brenham.

Cosmogenic Aluminum-26–The ^{26}Al activity in Brenham is in equilibrium so its activity in any particular phases directly yields its production rate. The measurement of cosmogenic ^{26}Al in the stone fractions provides the ^{26}Al production rate from the targets Fe and Si. In principle, ^{26}Al is produced from the targets P and S, however, these elements have extremely low concentrations in olivine. In iron meteorites, the P concentration is between 0.01 and 1% (Buchwald, 1975). Even though P is a trace constituent of iron its higher production rate, relative to Fe, necessitates consideration of this production pathway. The $P(^{26}Al)_P/P(^{26}Al)_{Fe}$ is given by the relation

$$P\left(^{26}\mathrm{Al}\right)_P / P\left(^{26}\mathrm{Al}\right)_{Fe} = (56/31)^{1/3} \times (34/9)^{k_2} \qquad (14)$$

An estimate for the importance of this reaction can be made by considering ^{21}Ne productions. Both ^{21}Ne and ^{26}Al are produced from ^{31}P, with ΔA's of 14 and 9, respectively. The production rate ratio of ^{21}Ne from P to that from Fe, $P(^{21}Ne)_P/P(^{21}Ne)_{Fe}$, is lower by a factor of 2–3 than the corresponding ratio of ^{26}Al. The production rate ratio $P(^{21}Ne)/P(^{26}Al)$ in phosphorus to that in Fe is estimated by the relation $(39/34 \times 9/14)^{k_2}$, where $k_2 = 3$–3.5. Brenham metal is known to contain 0.14% P, low but not unusual among medium octahedrites, IIIA group (Buchwald, 1975). The low P abundance, when combined with the low production rate of ^{21}Ne from P, eliminates the consideration of this production

TABLE 7. Meteoritic potassium in stone phase of Brenham.

	$^{40}Ar_s$ Observed (10^{-8} cm^3/g)	$(^{40}Ar/^{36}Ar)_s$ Observed	Cosmogenic $(^{38}Ar/^{36}Ar)_m$ Observed	Estimation using model	$(^{40}Ar/^{36}Ar)_s$ Air + cosmog. non-radiog.*	Potassium in stone (ppb)
N94†	14.4	60.94	1.596	1.604	59.83	35 ± 17‡
N91†	16.0	45.22	1.606	1.615	45.13	4 ± 17
UCSD86	14.1	88.10	–	–	87.84	5
AMNH880	7.29	150.7	1.670	1.665	148.32	15 ± 3
Reed 1	16.9	147.6	–	1.672	147.37	3 ± 5
Reed 2	9.47	141.7	1.682	1.672	140.75	9 ± 2
Reed 3	13.10	132.5	–	1.672	133.08	–8 ± 5
HJ91	11.0	184.5	1.673	1.672	189.72	–35 ± 4
H49.236-2	14.5	252.8	1.690	1.694	253.4	–4 ± 5
AMNH881	7.05	290.1	1.750	1.746	289.4	2 ± 14
Ward LJS	96.0	295.2	1.733	1.732	295.4	–8 ± 62
Ward 10.50	40.9	328.3	–	1.761	292.6	590 ± 24§
Ward 10.50	21.1	295.5	1.762	1.761	293.9	15 ± 13
Ward 10.50	39.3	297.5	–	1.761	295.3	39 ± 23

Potassium (ppb) = $((^{40}Ar/^{36}Ar)_{obs} - (^{40}Ar/^{36}Ar)_{non\text{-}radiogenic}) \times (^{36}Ar)_s/0.00754$, assumed 4.5 Gyr for solidification age.
A direct NAA method for ^{41}K also gave low potassium contents in stone phase of Brenham.
The lowest in AMNH881, 3 ppb K and 10–20 ppb K in other fragments (Ebihara, pers. comm., 1998).
*Non-radiogenic $(^{40}Ar/^{36}Ar)_s = 296 \times (1 - ((^{38}Ar/^{36}Ar)_s - 0.188)/((^{38}Ar/^{36}Ar)_m - 0.188))$.
†Ignored cosmogenic ^{40}Ar
‡Calculated value in N94 is apparently too high, caused by cosmogenic component.
§Contaminated with radiogenic component. See also Table 4, showing a high radiogenic ^4He.

pathway for Brenham. Exceptions to this rule can be seen for those samples having higher shielding (AMNH880 and H49.236) in which case the production of ^{26}Al from P is estimated to be 10% of that from Fe. For iron meteorites classified within groups IIB and IIIB the phosphorus contents are close to 1%. The production of ^{21}Ne from P is sufficient to perturb the ^{4}He/^{21}Ne ratio under heavier shielding conditions for such class of iron meteorites.

Shielding Independent Radionuclide Pairs–It is noteworthy that two high-energy products, ^{26}Al and ^{10}Be, are produced with a constant value, $P(^{26}\text{Al})/P(^{10}\text{Be}) = 0.71 \pm 0.05$, throughout the entire range of shielding conditions observed in Brenham metal phases. The ratios found in Brenham are consistent with many measurements in other iron meteorites (*e.g.*, Aylmer *et al.*, 1988; Lavielle *et al.*, 1999; Nagai *et al.*, 1993). In fact, this production rate ratio, found in iron meteorites nearly equals the ratio of these two nuclide's high-energy proton cross sections (*e.g.*, Dittrich *et al.*, 1990; Michel *et al.*, 1995, 1997). These observations clearly confirm our hypothesis of a single-stage irradiation history for Brenham.

Another radionuclide pair that is independent of shielding is the ^{36}Cl-^{36}Ar pair (Lavielle *et al.*, 1999). In this reaction 84% of the ^{36}Ar is derived from decay of ^{36}Cl. However, successful application of this pair requires correction for the ^{36}Cl that decayed during Brenham's 20 000 year terrestrial residence; this amounts to 5% of the total ^{36}Cl inventory.

Shielding Dependent Parameters–A key element in the reconstruction of cosmic-ray exposure histories is the extent to which any given sample has been shielded from cosmic rays. The semi-empirical approach presented herein parameterizes this physical quantity. However, in many instances it is possible to replace these parameters with ratios of cosmogenic nuclides. A significant goal of this work then is the verification of the utility of these measured ratios as proxies for shielding. The premier example of a shielding parameter based on cosmogenic nuclide ratios is the ^{4}He/^{21}Ne ratio in metal. Table 8 summarizes both the measured and the predicted ^{4}He/^{21}Ne ratios using several nuclide pairs in the metal and stone phases. The predictions are based on our determination of the shielding parameter, k_2. The salient observation from this data set is that the predicted ^{4}He/^{21}Ne ratios, based on cosmogenic ^{3}He, are in general consistent with measured values. These results validate the use of our semi-empirical relationships for production rates and the specific selection of the ^{4}He/^{21}Ne ratio as a shielding parameter for iron meteorites. The measured ^{4}He/^{21}Ne ratios of samples HJ91 and H49.236-1 display some deviations from the predicted values. It is not possible to ascertain whether these are the result of inaccurate measurement, improper sampling preparations, or alteration of cosmogenic nuclide record by terrestrial weathering. It may be true that the disturbances were considerable because the proper blank subtractions could not be made for the extremely low $^{21}\text{Ne}_m$ contents in metal.

TABLE 8. Production rate ratios of ^{4}He/^{21}Ne in Brenham metal.

	Measured	Estimated						Measured	Model values from $^{3}\text{He}_m$†		
	$(^{4}\text{He}/^{21}\text{Ne})_m$	$(^{4}\text{He}/^{36}\text{Ar})_m$*	$(^{3}\text{He}/^{21}\text{Ne})_s$	$(^{53}\text{Mn}/^{36}\text{Cl})_m$	$^{26}\text{Al}_s/^{26}\text{Al}_m$	$^{10}\text{Be}_s/^{10}\text{Be}_m$	Average	$^{3}\text{He}_m$ (10^{-8} cm^3/g)		k_1	k_2
$\Delta A'/\Delta A'$	14/39	14/24	22/12	8/24	7/34	11/28					
fff	18.3/1	18.3/0.78	27/1.6	0.9/0.64	0.09/0.23	0.13/0.18					
N94	275	245	259	274	320	260	276 ± 23	58.02	280	53.0	2.71
N91	329	282	331	237	341	267	298 ± 42	45.03	300	51.4	2.76
AMNH880	436	449	(704)	389	444	454	435 ± 26	7.48	415	17.7	3.14
Reed 2	450	424	400	410	435	429	425 ± 18	6.08	420	17.7	3.14
Reed 3	–	–	294	372	343	394	351 ± 43	–	–	17.4	3.14
HJ91	537	470	541	406	508	423	481 ± 57	4.15	450	13.4	3.19
H49.236-1	399	392	386	–	–	–	–	2.89	460	9.45	3.24
H49.236-2	468	401	(279)	346	428	458	420 ± 49	2.35	480	9.45	3.24
AMNH881	723	875	714	(993)	915	(1370)	807 ± 103	0.21	690	2.3	3.55
Ward LJS	553	534	426	619	587	803	587 ± 125	0.18	710	2.0	3.60
Ward 10.50	582	693	841	(230)	–	–	705 ± 130	0.13	740	1.7	3.65

A small correction was made for $^{21}\text{Ne}_m$ and $^{26}\text{Al}_m$ by subtracting contributions from phosphorus, 0.14% P, in metal.
*For example $\log(^{4}\text{He}/^{21}\text{Ne})_m = \log((^{4}\text{He}/^{36}\text{Ar})_m/(18.3/0.78))/\log(24/14) \times \log(39/14) + \log(18.3)$, because, $P(^{4}\text{He})_m = 18.3 \times k_1 \times (14)^{-k_2}$ (atom/min g), $P(^{21}\text{Ne})_m = 1 \times k_1 \times (39)^{-k_2}$, $P(^{36}\text{Ar})_m = 0.78 \times k_1 \times (24)^{-k_2}$ then, $P(^{4}\text{He}/^{21}\text{Ne})_m = (18.3/1) \times (39/14)^{k_2}$, $\log P(^{4}\text{He}/^{21}\text{Ne})_m = k_2 \times \log(39/14) + \log(18.3)$, $k_2 = \log((P(^{4}\text{He})_m/18.3)/(P(^{36}\text{Ar})_m/0.78))/\log(24/14)$.
†$P(^{4}\text{He}/^{21}\text{Ne})_m$ estimated by smoothing with an empirical relation: $(^{4}\text{He}/^{21}\text{Ne})_m = 546 \times (^{3}\text{He})_m^{-0.155}$ where $(^{3}\text{He})_m$ is in unit of 10^{-8} cm^3/g.

Production Rates and Exposure Ages–Table 9 summarizes a comparison of measured and estimated cosmogenic nuclide production rates for Brenham. The two parameters, ΔA' and *f*, are listed in the table. Nagai *et al.* (1993) derived ΔA' and *f* for $^{10}Be_m$ as 22 and 0.11, respectively. For this work more appropriate values, ΔA' = 28 and *f* = 0.18, are applied. The stable nuclide production rates were estimated based on exposure age of 156 Myr (see Table 10). Table 10 presents the exposure age determinations. These ages are determined by utilizing suitable pairs of stable and radionuclides. Shielding independent and shielding corrected exposure ages are shown in the table. Two sets of parameters, ΔA' and *f* or production rate ratio (case of shielding independent age), for each nuclide pair are listed in the table. The ^{36}Cl-^{36}Ar exposure age is known to be the most reliable and shielding independent method for iron meteorites or metallic phases (*e.g.*, Lavielle *et al.*, 1999; Schaeffer and Heymann, 1965). The exposure age, T_{36-36}, was calculated as following based on the production rate ratio, $P(^{36}Cl)/P(^{36}Ar)$, of 0.835 (Lavielle *et al.*, 1999),

$$T_{36-36} = 511 \times P(^{36}Cl)/P(^{36}Ar) \times [^{36}Ar]/[^{36}Cl] \quad (15)$$

where $[^{36}Ar]$ and $[^{36}Cl]$ are the ^{36}Ar (10^{-8} cm^3/g) and ^{36}Cl (dpm/kg) concentrations measured in the same sample, respectively. The concordancy of the exposure ages independent of the shielding conditions validates the constancy of the production rate ratio of $^{36}Ar/^{36}Cl$ over a wide range of shielding. Exposure ages based on the ^{10}Be-^{21}Ne and ^{26}Al-^{21}Ne pairs (for the metal phases) have also been computed. The formulae for ^{10}Be-^{21}Ne and ^{26}Al-^{21}Ne methods are similar in form to Eq. (15), only requiring the appropriate production rate ratios. The constant production rate ratios ($P(^{26}Al)/P(^{21}Ne)$ = 0.35 and $P(^{10}Be)/P(^{21}Ne)$ = 0.5) used here are slightly lower than previous estimates (*e.g.*, Hampel and Schaeffer, 1979; Lavielle *et al.*, 1999). The calculated exposure ages for all shielding conditions were in excellent agreement with each other and those based on the ^{36}Cl-^{36}Ar method. We also calculated ^{10}Be-^{21}Ne exposure ages in the silicate phase using the method of Graf *et al.* (1990). These ages showed

TABLE 9. Comparison of measured and estimated cosmogenic nuclide production rates for Brenham.

	^3He_s	^4He_s	$^{21}Ne_s$	$^{38}Ar_s$	^3He_m	^4He_m	$^{21}Ne_m$	$^{36}Ar_m$	$^{38}Ar_m$	$^{10}Be_s$	$^{26}Al_s$	$^{10}Be_m$	$^{26}Al_m$	$^{36}Cl_m$	$^{53}Mn_m$
ΔA'	22	13	12	22	22	14	39	24	22	11	7.5	28	34	24	8
f	27	40	1.6	0.1	16.7	18.3	1	0.78	1	0.13	0.09	0.18	0.23	0.64	0.9
Meas./Estim.*	1.07	1.03	1.05	1.04	1.01	0.97	1.04	1.02	1.03	1.05	1.02	1.07	0.96	1.08	1.02
Deviation (%)*	12	15	17	26	13	11	16	11	11	11	9	16	11	9	14

*Averaged values and standard deviation of (measured production rate)/(model estimation) for N94 through Wards, or shielding indicator, $(^4He/^{21}Ne)_m$ = 280–720. Data of Reed 3 and H49.236-1 were omitted from the calculation.

TABLE 10. Exposure ages of Brenham obtained from radionuclide and stable nuclide pairs.

Sample	Shielding independent exposure ages (Myr)			Shielding corrected exposure ages (Myr)			
	$^{36}Ar/^{36}Cl$	$^{21}Ne_m/^{10}Be_m$	$^{21}Ne_m/^{26}Al_m$	$^{38}Ar_m/^{10}Be_m$	$^{21}Ne_s/^{10}Be_s$	$^{21}Ne_m/^{26}Al_m$†	$^4He_m/^{53}Mn_m$
ΔA'/ΔA'	24/24	39/28	39/34	22/28	12/11	39/34	14/8
P/*P* or *f*/*f**	0.835	0.5	0.35	1/0.18	1.6/0.13	1/0.23	18.3/0.9
N94	160	182	179	156	171	188	144
N91	144	152	148	145	167	158	164
AMNH880	156	177	164	172	167	194	165
Reed average	151	160	154	150	164	177	141
H.J91	153	140	140	158	193	171	162
H49.236	164	166	137	185	143	143	177
AMNH881	(125)	173	162	(209)	107	(239)	(87)
Ward LJS	167	164	(121)	169	140	(175)	(119)
Ward 10.50	(95)	–	–	–	140	–	147
Average age (Myr)	156 ± 8	164 ± 14	155 ± 15	162 ± 14	155 ± 25	172 ± 19	157 ± 13

Ages in parentheses were not included for calculation of average age due to the large experimental errors. The radionuclide activities were corrected at the time of fall using 20 kyr of terrestrial age.

*Production rate ratio, *P*(stable nuclide)/*P*(radionuclide), for shielding independent exposure ages and *f*(stabel nuclide)/*f*(radionuclide) for shielding corrected exposure ages.

†A small correction was made for $^{26}Al_m$ by subtracting contributions from phosphorus, 0.14% P, in metal.

considerable scatter from sample to sample, more than ±30% in many instances.

Shielding corrected exposure ages were computed using the production rate ratios that were calculated by the semi-empirical relations. The shielding parameters, k_1 and k_2, used in the calculation are listed in Table 8. The calculated four exposure ages for all shielding conditions were in good agreement with each other and those based on the ^{36}Cl-^{36}Ar method. The shielding corrected ^{10}Be-^{21}Ne exposure ages in the silicate phase were better agreement than that obtained by the method of Graf *et al.* (1990).

The concordancy of the exposure ages discussed above allows us to conclude that, spanning a time-frame of 1 to ~5 Myr, the production rate ratios (^{10}Be/^{26}Al/^{36}Cl) have been constant. This can only occur if both the shielding conditions of these samples as they resided within Brenham and the galactic cosmic-ray flux remained constant during the last 5 Myr.

The ^{10}Be/^{36}Cl ratio is now used as a sensitive indicator of terrestrial age (Nishiizumi *et al.*, 1997a). The utility of this technique is based on the constancy of this production rate ratio or, in instances where unusual shielding conditions occur, predictable deviations from the nominal value. Under most shielding conditions this ratio is constant, but like the ^{38}Ar/^{36}Ar ratio, deviations do occur. For the lowest shielding conditions a ^{10}Be/^{36}Cl ratio of ~4 is measured, whereas at the other extreme, in heavily shielded metal samples, ratios of 5.5–6 were observed.

Radionuclides in Comparisons with Lunar Surface Samples

Radionuclide production in the lunar regolith, as sampled in lunar cores, is similar in many aspects to that in Brenham. This similarity provides a means to relate the shielding indices derived from Brenham to absolute shielding depth (g/cm^2). The depth profiles of cosmogenic radionuclides in the Apollo 15 long drill core that was recovered from near the surface of the Moon extend to 400 g/cm^2 depth (Imamura *et al.*, 1973; Nishiizumi *et al.*, 1984b,c, 1997b). Measurement of neutron-capture products, such as Gd and Sm, suggest a steady-state irradiation (Russ *et al.*, 1972). The activities of ^{53}Mn in this core are saturated; these activities are close to those found in those samples identified as near the surface of Brenham. In the lunar core, 170 dpm ^{53}Mn/kg Fe and 7 dpm ^{10}Be/kg were found at 150 g/cm^2 (Imamura *et al.*, 1973; Nishiizumi *et al.*, 1984b). In Brenham, 170–120 dpm ^{53}Mn/kg metal and 9–8 dpm ^{10}Be/kg stone were observed in N94 and N91 (Table 6).

The semi-empirical technique used for Brenham can also be applied to lunar surface samples. We will first determine the shielding parameters (*e.g.*, the shielding indices for the lunar core samples of known shielding). The correspondence between the shielding parameters and depth for the lunar samples can be used to determine shielding depths for the Brenham samples.

Since cosmogenic nuclides produced by higher energy reactions in lunar soil are scarce, the shielding index, k_2, is estimated independently using the ^{53}Mn/^{10}Be ratio in silicates. This estimation has a 10% uncertainty. For samples at the bottom of the Apollo 15 core, 400 g/cm^2, a value for k_2 of 3.0–3.1 was obtained. The robustness of this estimation is less than satisfactory owing to the similarity in the ΔA's of the products, but if we take $k_2 = 3.05$ at $d = 400$ g/cm^2, the empirical relation $k_2 = 1.37 \times d^{0.134}$ is obtained. Figure 3 presents a comparison of the exposure depths between Brenham and the lunar core samples. The ^{10}Be (Nishiizumi *et al.*, 1984b) and ^{53}Mn (Imamura *et al.*, 1973) in the Apollo 15 deep core are plotted as a function of the depth on the Moon. As was done in Brenham, the shielding parameter is estimated using the ratio of two cosmogenic nuclides, specifically the ratio of ^{53}Mn in Fe to ^{10}Be in the silicates between 100 and 400 g/cm^2.

To facilitate a direct comparison, the ^{53}Mn activities found in the metal phase of Brenham are modified slightly since Brenham metal contains 10% Ni whereas Ni concentration is negligible in lunar samples. The ^{10}Be found in lunar silicates can be compared to that in Brenham olivines after some minor corrections. The major target element for the production of ^{10}Be is oxygen. The oxygen concentration in lunar samples and Brenham olivine is 44% and 50%, respectively. We estimated the ^{10}Be production rate of Brenham olivine to be about 10–20% higher than that of lunar soils. There is no rigorous manner to be more precise about the difference. For our calculations we assume a +10% modification. After these minor corrections, we found that the shielding depths of the top three Brenham samples, N94, N91, and AMNH880, correspond to an equivalent of 150–400 g/cm^2 in the lunar regolith. The relationship between depth and the shielding indicator as given by the ^{4}He/^{21}Ne ratio is

$$d = 7.34 \times 10^{-5} \times (^4\mathrm{He}/^{21}\mathrm{Ne})_m^{2.58} \text{ g/cm}^2 \qquad (16)$$

This relationship can be compared with the empirical relation between k_2 and d as determined from the lunar core samples. Deviations between these two are small, even in regions of higher shielding. Extrapolation of these relations enables us to reach deeper than 800 g/cm^2 (Fig. 3). This relation, however, does not describe cosmogenic nuclide production in near-surface region of <150 g/cm^2. Our measurements for Brenham are consistently higher in activity than the corresponding lunar samples. Comparisons of depth and shielding indices have ambiguities arising from two sources: (1) the effects of bulk chemical compositions on productions, (2) deviations in Brenham from a strict 2π geometry.

Geometry and Preatmospheric Size of Brenham

Based on our measurements, and the comparison with the lunar core samples for shielding <150 g/cm^2, we conclude that the Brenham meteoroid might not be as large as originally believed, and the geometry may not be strictly 2π (Nagai *et al.*, 1993). Fragments of the Antarctic iron meteorites, Derrick

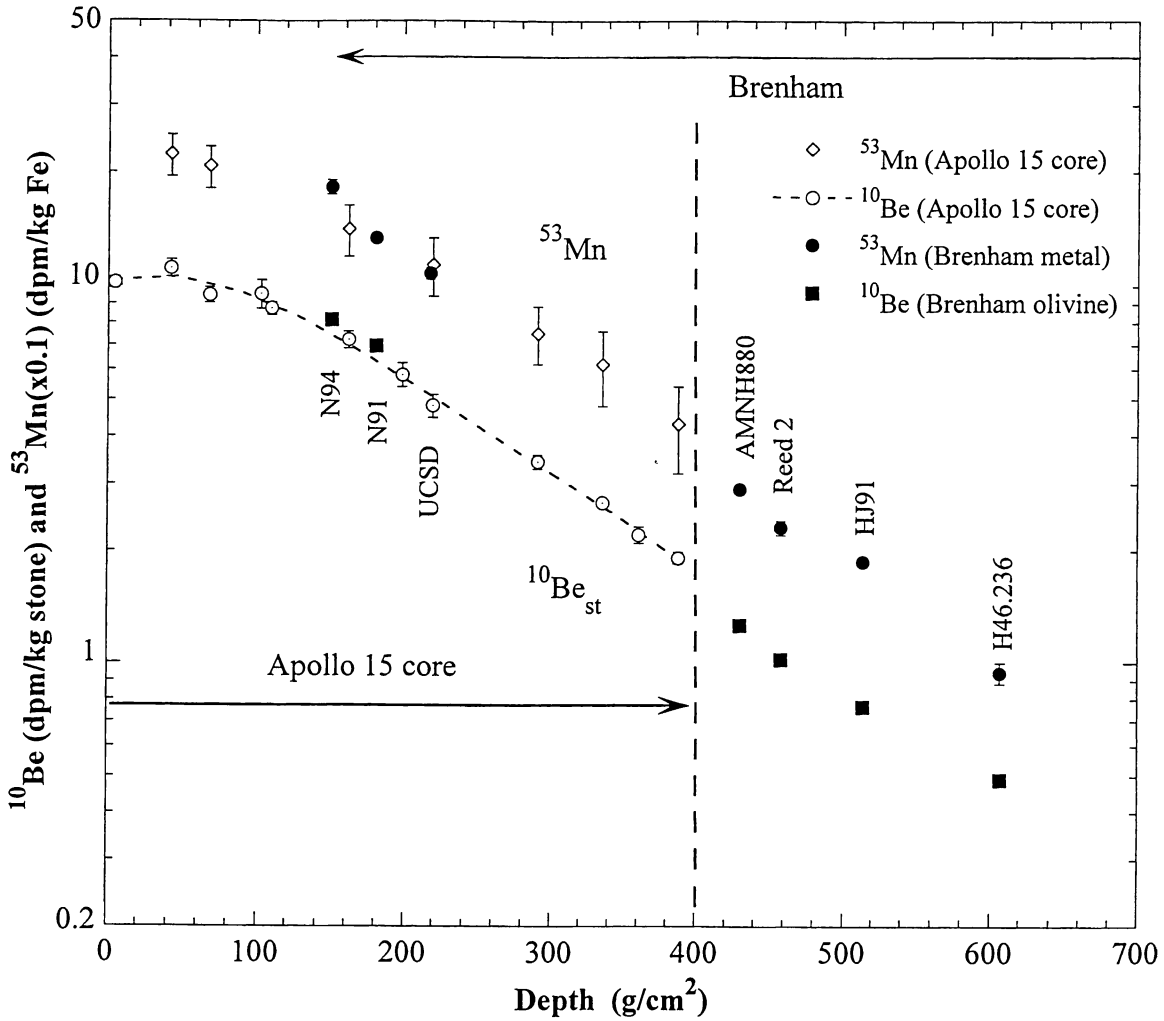

FIG. 3. Comparison of radionuclide production in lunar surface core and in Brenham. The depth profile data of ^{53}Mn and ^{10}Be are plotted for Apollo 15 core and Brenham that are discussed in Table 9. The data for deeper interior samples, AMNH881 and Ward, are not plotted. Those near-center samples may represent 4π geometry rather than 2π.

Peak (DRP) 78002-9 (Nishiizumi *et al.*, 1986) have similar radionuclide activities as Brenham metals.

Although the total mass of the Brenham pallasite cannot be determined from the recovered mass, estimates based on the collected fragments indicate a mass of more than 4 tons. Additionally, prehistoric samples of "Hopewell Mounds" have been identified as metallic parts of Brenham (Wasson and Sedwick, 1969). More recent recoveries of the fragments, HJ91, may also be added. Some of the fragments in our collections must have originated not far from the center of the meteoroid. The deepest sample, Ward, resided at an estimated depth of ~1600 g/cm^2. Assuming a mean density of Brenham of 5 g/cm^3 (±10%), the minimum pre-atmospheric mass can be estimated at 500 ± 100 tons, or 6 m in diameter. Unfortunately the metal fractions are predominant in some fragments, and the representative density of the meteoroid cannot be estimated well. According to Nininger (1952), the size of the main crater was "36 ft × 55 ft" in the form of an ellipse.

Effect of Bulk Chemistry on Production Rates

Possible matrix effects due to the bulk chemical composition should be considered. Although these effects have been discussed there is little quantitative information regarding their effects in large objects like the Brenham meteorite. Masarik and Reedy (1994) calculated elemental production rates of cosmogenic nuclides in different type of meteorites. Their calculation indicates that the ^{53}Mn production rates of iron and stony iron meteorites are more than 10–20% higher than those of stony meteorites. This circumstance arises because the production rates increase with Fe concentration. The same tendency has been reported for the production rates of stable nuclides in meteorites with different chemical compositions (Begemann and Schultz, 1988; Jentsch and Schultz, 1996).

It may also be noted that the maximum production rates of ^{53}Mn in relatively small iron meteorites, such as Dayton and Udei Station, have been observed at ~600 dpm/kg Fe

(Nishiizumi, 1978, 1991). The same can be said in large and long-exposed chondrites, such as Yamato-74192 (H6) (Nishiizumi *et al.*, 1980). There is also a considerable wealth of cosmogenic nuclide data from very large iron meteorites, such as Canyon Diablo (Merchel *et al.*, 2001; Michlovich *et al.*, 1994), Cape York, DRP 78001-9 (Nishiizumi *et al.*, 1987), Gibeon, and Sikhote-Alin and it is useful to compare radionuclides in these samples with Brenham. In Sikhote-Alin the highest value is reported to be 300 dpm ^{53}Mn/kg (Alexeev *et al.*, 1987, and our unpubl. data). This value is unequivocally higher than maximum galactic cosmic-ray produced ^{53}Mn activity, 220–240 dpm/kgFe, found in lunar cores at 30–100 g/cm^2 (Imamura *et al.*, 1973, 1974; Nishiizumi *et al.*, 1983). This sample suggests some positive matrix effects in near surface of meteorites. If this is the case, the depth, d, estimated in above relation as a function of shielding, should be shifted by about +30 g/cm^2, which corresponds, to a +20% effect for each fragment of Brenham listed in Fig. 3.

SUMMARY

Cosmogenic nuclides from both metal and silicate phases of the pallasite Brenham have been measured. These measurements have been interpreted within the framework of a parameterized semi-empirical model of cosmogenic nuclide production. Our results indicate that Brenham has undergone a simple single-stage exposure to cosmic rays. The concentrations of all cosmogenic stable and radionuclide measured in Brenham can be satisfactorily modeled using our approach and the predictions of the model are consistent with our own measurements and those of others.

Acknowledgments–We wish to thank J. R. Arnold for encouraging us for this line of study and for valuable discussions. The authors wish to thank J. R. Arnold, C. Moore, M. Prinz, and M. Shima for providing the Brenham samples. We wish to thank G. F. Herzog, R. C. Reedy, and R. Wieler for their thoughtful reviews of this paper. We have been helped by members of the AMS facilities at the University of Tokyo and the Lawrence Livermore National Laboratory. D. DePaolo graciously made a space available in his laboratory for sample processing at Berkeley. We also thank to Y. Li, K. Douzono, T. Asaka, Y. Anzai, Y. Nagano, and T. Oyama for a part of sample preparations. This work was partially supported by NASA grant NAG 5-4992. This work was also performed under the auspices of the US DOE by LLNL under contract W-7405-Eng-48.

Editorial handling: R. Wieler

REFERENCES

ALEXEEV V. A., MALISHEV V. V. AND LAVRUKHINA A. K. (1987) Spallogenic Mn-53 in some meteorites (abstract). *Lunar Planet. Sci.* **18**, 17–18.

AYLMER D., BONANNO V., HERZOG G. H., WEBER H., KLEIN J. AND MIDDLETON R. (1988) ^{26}Al and ^{10}Be production in iron meteorites. *Earth Planet. Sci. Lett.* **88**, 107–118.

BEGEMANN F. AND SCHULTZ L. (1988) The influence of bulk chemical composition on the production rate of cosmogenic nuclides in meteorites (abstract). *Lunar Planet. Sci.* **19**, 51–52.

BEGEMANN F., WEBER H. W., VILCSEK E. AND HINTENBERGER H. (1976) Rare gases and ^{36}Cl in stony-iron meteorites: Cosmogenic elemental production rates, exposure ages, diffusion losses and thermal histories. *Geochim. Cosmochim. Acta* **40**, 353–368.

BUCHWALD V. F. (1975) *Handbook of Iron Meteorites*. Univ. California Press, Berkeley, California, USA. 1418 pp.

DAVIS J. C. *ET AL.* (1990) LLNL/UC AMS facility and research program. *Nucl. Instrum. Methods* **B52**, 269–272.

DITTRICH B., HERPERS U., HOFMANN H. J., WÖLFLI W., BODEMANN R., LÜPKE M., MICHEL R., DRAGOVITSCH P. AND FILGES D. (1990) AMS measurements of thin-target cross sections for the production of ^{10}Be and ^{26}Al by high energy protons. *Nucl. Instrum. Methods* **B52**, 588–594.

EBERHARDT P. AND EBERHARDT A. (1960) Neon und andere Edelgase in Steinmeteoriten. *Helv. Phys.* **A33**, 593–594.

EBERHARDT P. AND EBERHARDT A. (1961) Ne in some stone meteorites. *Z. Naturforschg.* **16A**, 236–238.

GEISS J., OESCHGER H. AND SCHWARZ U. (1962) The history of cosmic radiation as revealed by isotopic changes in the meteorites and on the Earth. *Space Sci. Rev.* **1**, 197–223.

GRAF T., BAUR H. AND SIGNER P. (1990) A model for the production of cosmogenic nuclides in chondrites. *Geochim. Cosmochim. Acta* **54**, 2521–2534.

HAMPEL W. AND SCHAEFFER O. A. (1979) ^{26}Al in iron meteorites and the constancy of cosmic ray intensity in the past. *Earth Planet. Sci. Lett.* **42**, 348–358.

HONDA M. (1959) Cosmogenic potassium-40 in iron meteorites. *Geochim. Cosmochim. Acta* **17**, 148–150.

HONDA M. (1985) Production rate of cosmogenic helium isotopes in iron meteorites. *Earth Planet. Sci. Lett.* **75**, 77–80.

HONDA M. (1988) Statistical estimation of the production of cosmic-ray-induced nuclide in meteorites. *Meteoritics* **23**, 3–12.

HONDA M., UMEMOTO S. AND ARNOLD J. R. (1961) Radioactive species produced by cosmic rays in Bruderheim and other stone meteorites. *J. Geophys. Res.* **66**, 3541–3546.

IMAMURA M., FINKEL R. C. AND WAHLEN M. (1973) Depth profile of ^{53}Mn in the lunar surface. *Earth Planet. Sci. Lett.* **20**, 107–112.

IMAMURA M., NISHIIZUMI K., HONDA M., FINKEL R. C., ARNOLD J. R. AND KOHL C. P. (1974) Depth profiles of ^{53}Mn in lunar rocks and soils. *Proc. Lunar Sci. Conf.* **5th**, 2093–2103.

IMAMURA M., SHIMA M. AND HONDA M. (1980) Radial distribution of spallogenic K, Ca, Ti, V, Mn isotopes in iron meteorites. *Z. Naturforschg.* **35A**, 267–279.

JENTSCH O. AND SCHULTZ L. (1996) Cosmogenic noble gases in silicate inclusions of iron meteorites: Effects of bulk composition on elemental production rates. *J. Royal Soc. West. Australia* **79**, 67–71.

KOBAYASHI K. *ET AL.* (1997) Current status of the AMS system at the University of Tokyo. *Nucl. Instrum. Methods* **B123**, 107–111.

LAVIELLE B., MARTI K., JEANNOT J-P., NISHIIZUMI K. AND CAFFEE M. W. (1999) The ^{36}Cl-^{36}Ar-^{40}K-^{41}K records and cosmic ray production rates in iron meteorites. *Earth Planet. Sci. Lett.* **170**, 93–104.

MASARIK J. AND REEDY R. C. (1994) Effects of bulk composition on nuclide production processes in meteorites. *Geochim. Cosmochim. Acta* **58**, 5307–5317.

MATHEW K. J. AND BEGEMANN F. (1997) Solar-like trapped noble gases in the Brenham pallasite. *J. Geophys. Res.* **102**, 11 015–11 026.

MEGRUE G. H. (1968) Rare gas chronology of hypersthene achondrites and pallasites. *J. Geophys. Res.* **73**, 2027–2033.

MERCHEL S., FAESTERMANN T., HERPERS U., KNIE K., KORSCHINEK G., LEYA I., LIPSCHUTZ M. E. AND MICHEL R. (2001) Cosmogenic nuclides in iron meteorites: Challenging Canyon Diablo (abstract). *Meteorit. Planet. Sci.* **36 (Suppl.)**, A132.

MICHEL R., DRAGOVITSCH P., CLOTH P., DAGGE G. AND FILGES D. (1991) On the production of cosmogenic nuclides in meteoroids by galactic protons. *Meteoritics* **26**, 221–242.

MICHEL R. *ET AL.* (1995) Nuclide production by proton-induced reactions on elements (6 = Z = 29) in the energy range from 800 to 2600 MeV. *Nucl. Instrum. Methods* **B103**, 183–222.

MICHEL R. *ET AL.* (1997) Cross sections for the productions of residual nuclides by low- and medium-energy protons from the target elements C, N, O, Mg, Al, Si, Ca, Ti, V, Mn, Fe, Co, Ni, Cu, Sr, Y, Zr, Nb, Ba, and Au. *Nucl. Instrum. Methods* **129**, 153–193.

MICHLOVICH E. S., VOGT S., MASARIK J., REEDY R. C., ELMORE D. AND LIPSCHUTZ M. E. (1994) Aluminum 26, ^{10}Be, and ^{36}Cl depth profiles in the Canyon Diablo iron meteorite. *J. Geophys. Res.* **99**, 23 187–23 194.

MILLARD H. T. J. (1965) Thermal neutron activation: Measurement of cross section for manganese-53. *Science* **147**, 503–504.

MIURA Y. N. (1995) Studies on differentiated meteorites: Evidence from ^{244}Pu-derived fission Xe, ^{81}Kr, other noble gases and nitrogen. PhD. thesis, University of Tokyo, Tokyo, Japan. 183 pp.

MORGAN J. W. AND LOVERING J. F. (1973) Uranium and thorium in achondrites. *Geochim. Cosmochim. Acta* **37**, 1697–1707.

NAGAI H., HONDA M., IMAMURA M. AND KOBAYASHI K. (1993) Cosmogenic ^{10}Be and ^{26}Al in metal, carbon, and silicate of meteorites. *Geochim. Cosmochim. Acta* **57**, 3705–3723.

NAGAI H., KOKUBO M., KOBAYASHI T. AND HONDA M. (1999) Cosmogenic ^{10}Be and ^{26}Al in iron meteorites and the inclusions (abstract). *Antarctic Meteorites* **24**, 116–118.

NAGAO K. (1994a) Noble gases in hosts and inclusions from Yamato-75097(L6), -793241(L6) and -794046(H5). *Proc. NIPR Symp. Antarct. Meteorites* **7**, 197–216.

NAGAO K. (1994b) Xe isotope compositions in silicate phase of the Brenham pallasite: A possible carrier of U-Xe (abstract). In *Intl. Workshop Noble Gas Geochemistry Cosmochemistry*, pp. 4–5. Yamada Conference 38, Japan.

NAGAO K., MIURA Y. N., HONDA M. AND NAGAI H. (1996) Noble gases in metal phase of the Brenham pallasite (abstract). *Antarctic Meteorites* **21**, 128–130.

NININGER H. H. (1952) *"Out of the Sky", An Introduction to Meteoritics.* Dover Publ. Co., Mineola, New York, USA. 336 pp.

NISHIIZUMI K. (1978) Cosmic ray produced ^{53}Mn in thirty-one meteorites. *Earth Planet. Sci. Lett.* **41**, 91–100.

NISHIIZUMI K. (1987) ^{53}Mn, ^{26}Al, ^{10}Be, and ^{36}Cl in meteorites: Data compilation. *Nucl. Track Radiation Meas.* **13**, 209-273.

NISHIIZUMI K., MURRELL M. T., ARNOLD J. R., IMAMURA M. AND HONDA M. (1980) Cosmogenic ^{53}Mn survey of Yamato meteorites. *Mem. Natl. Inst. Polar Res., Spec. Issue* **17**, 202–209.

NISHIIZUMI K., MURRELL M. T. AND ARNOLD J. R. (1983) ^{53}Mn profiles in four Apollo surface cores. *Proc. Lunar Planet. Sci. Conf.* **14th**, *J. Geophys. Res.* **88**, B211–B219.

NISHIIZUMI K., ARNOLD J. R. AND ELMORE D. (1984a) Cosmogenic nuclides in peculiar meteorites (abstract). *Meteoritics* **19**, 283.

NISHIIZUMI K., ELMORE D., MA X. Z. AND ARNOLD J. R. (1984b) ^{10}Be and ^{36}Cl depth profiles in an Apollo 15 drill core. *Earth Planet. Sci. Lett.* **70**, 157–163.

NISHIIZUMI K., KLEIN J., MIDDLETON R. AND ARNOLD J. R. (1984c) ^{26}Al depth profile in Apollo 15 drill core. *Earth Planet. Sci. Lett.* **70**, 164–168.

NISHIIZUMI K., ELMORE D., KUBIK P. W. AND ARNOLD J. R. (1986) Depth variation in cosmogenic radionuclide production in very large meteorites: Allende and DRP78002-9 (abstract). *Lunar Planet. Sci.* **17**, 619–620.

NISHIIZUMI K., KLEIN J., MIDDLETON R. AND ARNOLD J. R. (1987) Long-lived cosmogenic nuclides in the Derrick Peak and Lazarev iron meteorites (abstract). *Lunar Planet. Sci.* **18**, 724–725.

NISHIIZUMI K., CAFFEE M. W., FINKEL R. C. AND ARNOLD J. R. (1991) ^{10}Be and ^{53}Mn in non-Antarctic iron meteorites (abstract). *Meteoritics* **26**, 379–380.

NISHIIZUMI K., CAFFEE M. W., JEANNOT J. P., LAVIELLE B. AND HONDA M. (1997a) A systematic study of the cosmic-ray-exposure history of iron meteorites: ^{10}Be-^{36}Cl/^{10}Be terrestrial ages (abstract). *Meteorit. Planet. Sci.* **32 (Suppl.)**, A100.

NISHIIZUMI K., FINK D., KLEIN J., MIDDLETON R., MASARIK J., REEDY R. C. AND ARNOLD J. R. (1997b) Depth profile of ^{41}Ca in an Apollo 15 drill core and the low-energy neutron flux in the Moon. *Earth Planet. Sci. Lett.* **148**, 545–552.

REEDY R. C., ARNOLD J. R. AND LAL D. (1983) Cosmic-ray record in solar system matter. *Ann. Rev. Nucl. Part. Sci.* **33**, 505–537.

RUSS G. P., III, BURNETT D. S. AND WASSERBURG G. J. (1972) Lunar neutron stratigraphy. *Earth Planet. Sci. Lett.* **15**, 172–186.

SCHAEFFER O. A. AND HEYMANN D. (1965) Comparison of ^{36}Cl-^{36}Ar and ^{39}Ar-^{38}Ar cosmic ray exposure ages of dated fall iron meteorites. *J. Geophys. Res.* **70**, 215–224.

SCHULTZ L. AND KRUSE H. (1989) Helium, neon, and argon in meteorites—A data compilation. *Meteoritics* **24**, 155–172.

SCOTT E. R. D. (1977) Pallasites—Metal composition, classification and relationships with iron meteorites. *Geochim. Cosmochim. Acta* **41**, 349–360.

STAUFFER H. AND HONDA M. (1962) Cosmic ray produced stable isotopes in iron meteorites. *J. Geophys. Res.* **67**, 3503–3512.

VOSHAGE H. AND FELDMANN H. (1979) Investigations on cosmic ray produced nuclides in iron meteorites, 3. Exposure ages, meteoroid sizes and sample depths determined by mass spectrometric analyses of potassium and rare gases. *Earth Planet. Sci. Lett.* **45**, 293–308.

WASSON J. T. AND SEDWICK S. P. (1969) Meteoritic material from Hopewell Indian Burial Mounds: Chemical data regarding possible sources. *Nature* **222**, 22–24.